Development and Testing of a UWB-Based Vehicle-to-Vehicle (V2V) Ranging System for Self-Propelled Rail Vehicles

Zezhou Wang, *Student Member, IEEE*, Predrag Spasojevic, *Member, IEEE*, Bryan W. Schlake, Ninad Mulay, Asim F. Zaman, and Xiang Liu

***Abstract*—The vehicle-to-vehicle (V2V) distance ranging system is a critical component of transportation automation, including the railroad industry. Although the mainline rail traffic is strictly regulated by sophisticated train control and dispatching systems, self-propelled rail vehicles, such as maintenance-of-way equipment and light rail vehicles, still rely on the safety discretion of human operators. To support both safety protection and autonomous operations for these vehicles, a fine-grained V2V ranging system is needed. This paper presents our design of a decentralized, high-resolution, short distance V2V ranging system based on ultra-wideband (UWB) impulse radio (IR) technology, implemented by commercial UWB sensors and customized algorithms. A field-testing case study has been conducted to validate the system performance on full-sized self-propelled rail vehicles. The test results quantified the concerned performance parameters of UWB technology for the chosen use case and proved both the operational concepts and the functional design in this study. Our methodology in algorithm design, field-testing, and analytical data metrics should provide implications for applying UWB to other evolving use cases of intelligent rail transportation. At the end of this paper, we evaluate the system capability using ROS simulation and conclude the lessons learned from the system design.**

***Index Terms*—Rail transportation, railroad communication, ultra-wideband technology, V2V ranging.**

Nomenclature

AV	Autonomous Vehicle.
CAS	Collision Avoidance System.
DOE	Department of Energy.
DOT	Department of Transportation.
DRTLS	Decawave Real Time Location System.
DSRC	Dedicated Short-Range Communications.
FCC	Federal Communications Commission.
FPS	Frame per Second.
FRA	Federal Railroad Administration.
GNSS	Global Navigation Satellite System.
GPS	Global Positioning System.
IR	Impulse Radio.
LiDAR	Light Detection and Ranging.
LOS	Line-of-Sight.
LRV	Light Rail Vehicle.
MOW	Maintenance-of-Way.
NLOS	Non-Line-of-Sight.
RF	Radio Frequency.
ROS	Robot Operating System.
RTD	Round-Trip Delay.
STD	Standard Deviation.
TDMA	Time Division Multiple Access.
TWR	Two-Way-Ranging.
UWB	Ultra-Wideband.

Manuscript received 3 June 2022; revised 11 January 2023 and 15 June 2023; accepted 2 October 2023. Date of publication 30 October 2023; date of current version 14 March 2024. This work was supported by the Federal Railroad Administration of the U.S. Department of Transportation, under Grant 693JJ619C000013. The review of this article was coordinated by Dr. Shiva Raj Pokhrel. *(Corresponding author: Xiang Liu.)*

Zezhou Wang, Asim F. Zaman, and Xiang Liu are with the Civil and Environmental Engineering, Rutgers University, New Brunswick, NJ 08854 USA (e-mail: zezhou.wang@rutgers.edu; asim.zaman@rutgers.edu; xiang.liu@rutgers.edu).

Predrag Spasojevic and Ninad Mulay are with the Electrical and Computer Engineering, Rutgers University, Piscataway, NJ USA (e-mail: spasojev@winlab.rutgers.edu; nmm213@scarletmail.rutgers.edu).

Bryan W. Schlake is with the Rail Transportation Engineering, Penn State Altoona, Altoona, PA 16601 USA (e-mail: bws14@psu.edu).

Digital Object Identifier 10.1109/TVT.2023.3327727

I. Introduction

Currently, most self-propelled rail vehicles require human operators to control their movements. Similar to the behaviors of single-lane highway traffic, these vehicles usually travel in a platoon on a rail track for the purposes of revenue moves, equipment repositioning, or roadway maintenance [1], [2]. Typical examples of these vehicles include trams/light rail vehicles (LRV) and maintenance-of-way (MOW) equipment. Common train control and signaling systems can only regulate the entire convoy, while the movements of individual vehicles are often neglected [1]. However, even with relatively-slow operating speeds, collisions inside the convoy may still happen from human errors, introducing property damage, casualties, and disruptions to normal operations.

Meanwhile, new concepts of autonomous railcars with independent motions have been proposed under trending studies. For example, the U.S. Department of Energy (DOE) recently awarded a research grant to a proposal for battery-powered autonomous "container railcar" to evaluate its system metrics and energy performance [3]. Such autonomous railcars, along with conventional self-propelled rail vehicles, desire an effective vehicle-to-vehicle (V2V) ranging system to provide both automation support and safety reinforcement.

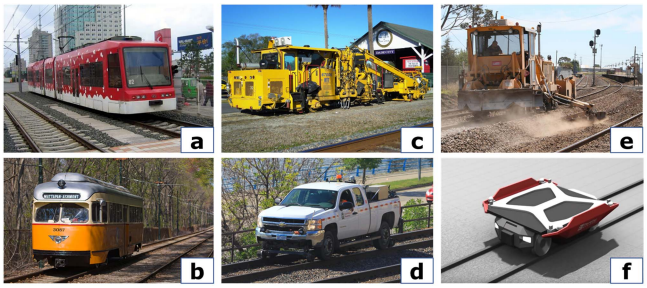

Fig. 1. Examples of self-propelled rail vehicles: (a) LRV © Peter Li. (b) Street tram © Derek Yu. (c) Rail tamper © Harvey Henkelman. (d) Hi-rail truck © Michael Hicks. (e) Track ballast regulator © Marcus Wong. (f) Conceptual autonomous container railcar, image courtesy of Parallel Systems [3].

Recent developments in ultra-wideband (UWB) impulse radio (IR) technology sparked many promising use cases in the transportation industry. Distributed UWB networks with ranging and cooperative positioning functions can reach centimeter-level accuracy without infrastructure support [4], [5]. Especially, the advantages of UWB technology perform in the very favor of V2V ranging applications, applicable to both highway autonomous vehicles (AV) and intelligent rail systems.

Besides its dominating advantage of ranging accuracy, UWB technology also has very flexible networking protocols, relaxed regulation, low-cost transceivers available in the market, low noise level to co-exist with traditional radios, and a growing community for technical support. Additionally, top-tier smartphone manufacturers such as Apple and Samsung have started to equip their products with UWB modules. The trend of UWB technology gives the reins to this research to consider its applications for rail industry innovations.

In this paper, we present the design of a UWB-based cooperative V2V ranging system for self-propelled rail vehicles, and tested it on a full-scale operational environment in collaboration with a major freight railroad company in the United States. In addition to the field-testing results, we assessed the system performance, stability, and design credibility using ROS simulations. Key contributions of this study are:

- The work demonstrates a novel methodology of migrating the off-the-shelf UWB positioning system to a multi-station, infrastructure-free, mutual V2V ranging system for rail vehicles. The adopted concepts and re-engineering processes shall inspire diversified applications in varied sectors.
- This paper showcases a pioneering design-build-test cycle of UWB in a rail-centric application environment.
- The work highlights a holistic package covering vehicles' mutual distance awareness, data exchange and networking, infrastructure independence, and deployment flexibility.
- The field-testing and simulation results validate our design's technological capability and versatility in assisting the selected rail use case. Operational scenarios that are impractical to test have been previewed in the simulations. During field tests, the system has achieved centimeter-level V2V ranging accuracy at a high rate of 10+ Hz in the absence of supplementary systems.
- The system assessment reveals both strengths and weaknesses in the current design, serving as the benchmark for relevant rail-UWB integrations, paving ways for additional use case formulation.

The paper is organized as follows:

First, we will conduct a literature review on the problem statement and related work. Then we elaborate on our engineering implementation, algorithms, and the field-testing processes for the proposed UWB V2V ranging system, followed by the analyses of test results. To further explore the global stability and convergence conditions, we replicate the system in an ROS simulator, operating it repetitively under extended scenarios. Finally, we discuss the work contribution, system integration options, lessons-learned, and potential improvements. The paper will be wrapped up with conclusions and expectations for future work.

II. Problem Statement

According to U.S. Federal Railroad Administration (FRA) accident records [6], a total of 122 accidents involving self-propelled rail vehicles took place from 2016 to 2021, leading to $11.3 million worth of damage and 382 injuries. FRA records indicated that human errors contributed to all of these accidents [7]. Mostly, the operators failed to stop the vehicle short of the adjacent one. The number of these accidents could be greatly reduced if a V2V distance ranging system were in place to improve the situational awareness of the operators.

In the global rail industry, the location and separation distance of trains are often inferred from centralized signaling and train control systems, using Global Navigation Satellite System (GNSS) or track-borne devices [8] (e.g., transponder or balise). However, GNSS will not operate inside tunnels or covered structures; its resolution also suffers in harsh satellite radio conditions, such as urban canyons and deep valleys, introducing complete signal loss or significant errors up to 40 meters [9], [10], [11]. Track-borne transponder technologies can be affected by cumulative errors from wheel creepage and slippage [12], and they only cover mainline tracks on primary corridors [13], [14] with the dependency on the cumbersome infrastructure.

For self-propelled on-track vehicles that are ubiquitous over the entire rail network, these said systems are insufficient to either guarantee accuracy, or provide decent reliability and functional coverage. Besides, to achieve timely safety responses, it is ideal to have vehicles exchange their high-resolution proximity information cooperatively with low latency. Therefore, a precise, distributed, lightweight, and infrastructure-free V2V ranging system is preferred over these centralized implementations [15]. Notably, self-propelled rail vehicles have relatively-slow operational speeds. Thus, such a V2V ranging system must outperform in short ranges with superior granularity. As further explained in Section III, UWB technology shall be qualified to supply all these features.

III. Related Work

To narrow our research scope and secure the choice of technology, we reviewed the related literature on general V2V ranging systems, categorized by two different methodologies: *egocentric*

ranging and *cooperative ranging*. These methodologies are also referenced in the trending research on highway autonomous vehicles (AV) ([10], [11]). In virtue of the analogical traffic pattern between self-propelled rail vehicles and highway automobiles [1], [2], we argue that such methodologies in highway studies are also applicable to our specific rail problem: because the fixed-guideway rail systems present a "better-controlled environment" [16] than roadway vehicular operations. Therefore, we can transfer the knowledge for AV studies to the rail-domain problem of self-propelled rail vehicles. The different approaches are reviewed below.

A. Egocentric Ranging

The egocentric approach does not require the ranging counterpart to participate in the ranging activities of the ego vehicle [11]. In practice, it covers not only applications of V2V, but also those of V2X (vehicle-to-everything). The frontier solutions often present low capital cost, fallback, and "turnkey" features [17], [18]. Egocentric implementations can be phased-in towards existing transportation systems, capable of handling miscellaneous objects. Currently, the technological bases of egocentric systems span over LiDAR (laser scanner, [19], [20], [21], [22]), mmWave radar ([20], [23], [24]), egocentric UWB radar ([25], [26], different from communication-based UWB), and camera vision perception ([27], [28]) for generic ranging and detection purposes. Typically, no communication links can be established between the ego vehicle and the ranging objects. Therefore, sole egocentric systems do not support mutual perception.

In the rail industry, two recent egocentric ranging studies have been carried out by the teams of Wang et al. Both systems implemented fused visual sensors [22], [24]. The proposal in [22] integrated machine vision with LiDAR for simultaneous object detection and distance measurement in subway. With rich tunnel and underground conditions, they achieved decimeter-level train-to-train ranging accuracy. In [24], they combined mmWave radar with computer vision AI to achieve egocentric positioning for trains, which can supply absolute positions for effective V2V ranging. However, the meter-level accuracy achieved in this study is suboptimal. For urban street trams, Lüy et al. designed a collision avoidance system based on LiDAR [29]. This system exposed the limitations of the relatively-low update rate and difficulties in object differentiation for LiDAR. Camera-based systems using machine vision 3D-reconstruction can be found in [1], [2], [30] for rail use cases. In these studies, ranging inputs depend on the calibration by the prior knowledge of fixed dimensions of common objects, such as the rail gauge. Unfortunately, these monocular approaches also suffered from low accuracy and indecisive perception.

Camera and LiDAR systems are susceptible to the environment, which generates noisy data that impair their ranging performance [11]. Egocentric UWB radar systems [25], [26] are no exception to this. Although UWB radar could potentially favor sensitive motion tracking with millimeter-level resolution ([31], [32]), the open-air harsh radio environment in railroad has a large amount of metal reflecting surfaces from vehicle bodies and the infrastructure, causing devastating difficulties of signal occlusion and reflection for ranging [33]. Besides, computer vision AI-based approaches often require expensive edge-computing power for real-time processing in onboard hosts [34], which limits both the scalability and the cost-effectiveness for many scenarios.

B. Cooperative Ranging

In cooperative ranging, vehicles exchange rich data through V2V communication links to share proximity perception. There are two general approaches to cooperative V2V ranging in trending studies: absolute position difference and radio round-trip delay (RTD) calculation.

In absolute position difference, vehicles exchange absolute positions (e.g., geodetic coordinates) in real-time. This simultaneously requires a dependable V2V datalink and a dedicated positioning system, such as GNSS or track-borne referencing system in the rail industry. As stated in Section II, the inputs from GNSS and track-borne transponders present limitations in accuracy or availability. As an example, the team of Do et al. integrated GPS with IEEE 802.11p DSRC links for simultaneous localization, ranging, and communication in transit street trams [35]. Due to GPS-dependency, the system only functions in open-air areas, and their update rate was limited to 2 Hz in the absence of high-end GNSS modules.

In radio RTD approaches, accurate ranging must claim exceptional temporal resolution of the radio in order to calculate precise propagation time. Traditional narrow-band radio frequency systems such as Bluetooth and Wi-Fi cannot provide such resolution. With large bandwidth and extremely short impulses, communication-based UWB-IR technology achieves sub-nanosecond level in time resolution [36]. This advantage supports centimeter-level accuracy in distance ranging, making it the primary technology in RTD-based ranging methods in recent years [37], [38]. The wide bandwidth also supports sufficient data throughput to maintain both a high ranging update rate (e.g., 10 Hz) and ad-hoc networking capabilities in the field [39]. These metrics rank in the top-tier of wireless solutions among the state-of-the-arts. In addition, UWB's independence from the positioning-infrastructure or communication-infrastructure granted itself desirable flexibility and freedom [40]. Therefore, with promising performance, a cooperative V2V ranging system supported by the standalone communication-based UWB-IR technology shall fulfill the specific research scope for self-propelled rail vehicles.

C. Research Novelty and Justification

In retrospect, although egocentric systems can detect heterogeneous objects with non-intrusive detection, it is always less definitive than a communication-based approach that can acquire ranging results directly from targets, enabling mutual presence awareness [41]. In our concerned scenarios of self-propelled rail vehicles, the fleet-level vehicle management under railroad companies guarantees the homogeneity of ranging participants. Therefore, a generic detection function is not imperative for our selected use case.

Commercial UWB-based cooperative V2V ranging systems in the rail industry came out as early as 2011 in the U.S., serving the collision avoidance function [42]. However, very

TABLE I
CROSS COMPARISON BETWEEN OUR STUDY AND RELATED V2V RANGING SYSTEMS

Technology	LiDAR and camera [23]	mmWave radar and camera [25]	Monocular camera [1], [2], [31]	Radar UWB [26], [27]	Absolute positioning difference [37]	**Communication UWB (our study)**
Methodology	Egocentric	Egocentric	Egocentric	Egocentric	Cooperative	Cooperative
V2V Ranging Accuracy	Decimeter (±0.3 m)	Meter (±5 m)	Meter or worse	Millimeter	Decimeter	**Centimeter (to be explained in result analyses)**
Update Rate	10 Hz max (limited by both sensor input rate and image processing power)	17 Hz max	5-10 Hz	50 Hz [43]	2 Hz	**10-40 Hz**
Environment Sensitivity	High (rely on favorable weather, lighting, or radio reflective conditions)				Medium‡	**Very low**
Max Range	240 m	250 m [44]	Depending on camera lens & track geometry	10-20 m	Depending on communication availability*	**40 m in field-testing 300 m in theory** [45]
V2V Communication Capability	No	No	No	No	**Yes (guaranteed vehicle mutual perception)**	
Infrastructure Dependency	No	No	No	No	Yes†	**No**

*Required V2V communication infrastructure: Wi-Fi mesh or cellular network (with opportunistic coverage). Ad-hoc V2V links do not require infrastructure.
† Infrastructure for position acquision: GNSS or track-borne transponders.
‡ GNSS is sensitive to covered structures. Transponder-based train localization is sensitive to slippery rails that cause wheel creepage.

few studies have been published in the scientific community detailing the engineering architecture, functional effectiveness, or performance metrics for UWB and its associated components. In recent years, UWB-IR transceiver cost has been dramatically reduced [43]. To understand the design methodology, system performance, integration options, and room for improvement of such UWB-rail applications, we present our design of a custom communication-based, cooperative UWB-IR RTD V2V ranging system, and have it successfully tested by self-propelled MOW rail vehicles. To tackle the niche problem, our study presents the following integrated advantages:

- High fidelity and excellence in ranging accuracy.
- A standalone, fully-distributed system that overcomes dependence on GNSS and infrastructure. This brings deployment flexibility, the ability to counter GNSS-denial, and cost-savings from peripheral systems.
- Mutual awareness and communication capabilities among rail vehicles for cooperativeness.

For the particular application, our work validates the technological feasibility, benchmarks UWB's performance, and raises the ranging accuracy and functional effectiveness to a higher bar. The methodology that migrates immobile UWB positioning design to a mobile ranging system is original. Specifically, we propose a novel solution to the accuracy impacts of vehicle dimensions under close proximity. This problem has not been addressed by current works in scope.

Compared to egocentric ranging, our work trades-off the detection heterogeneity with vehicle communication capability and environmental robustness. Within cooperative ranging methods, our standalone solution breaks the dependence on infrastructure support. The cross comparisons between the work in this paper and related V2V ranging implementations are summarized in Table I. To sum up, we advocate a communication-based, cooperative UWB V2V ranging approach for self-propelled rail vehicles with high fidelity, precise ranging accuracy, and simplicity attributive to the particular use case characteristics.

IV. SYSTEM IMPLEMENTATION AND METHODOLOGY

This section presents the details of architecture and algorithms in our UWB-IR V2V ranging system with an infrastructure-free, decentralized, and cooperative design for self-propelled rail vehicles. By design, each vehicle initiates ranging activities against the others within an established ad-hoc UWB network, and also responds to external ranging activities that come from the other vehicles.

Each vehicle's onboard subsystem consists of three major components: 1). two UWB master devices, 2). two UWB slave devices, and 3). one onboard computer. Each vehicle end ("A" or "B") is equipped with one master and one slave device, respectively. The placement of devices is quasi-centrosymmetric to the vehicle body, providing transceivers with the best line-of-sight (LOS) conditions among vehicles. Fig. 2 illustrates the system layout for an example of two adjacent vehicles.

During the UWB ranging operation, one vehicle measures the distance against another using UWB RTD calculation, powered by an auto-polling UWB-IR messaging service initiated from the master device to the slave device. When a master device transmits a timestamped UWB ranging request, it awaits any timestamped UWB response from slave devices. Thus, the RTD distance of one master/slave[1] pair is calculated by the two-way-ranging (TWR) expression (1):

$$\delta d = \frac{\left(T_{master}^{receive} - T_{master}^{transmit}\right) - \left(T_{slave}^{transmit} - T_{slave}^{receive}\right)}{2} \times c \tag{1}$$

where δd denotes the device-to-device distance during the ranging cycle. $T_{master}^{receive}$ denotes the timestamp when the master

[1]This project uses the conventional terms "master" and "slave" to denote primary and secondary UWB nodes respectively, with an implication of subordinative relationship. The terms are employed due to their widespread use and understanding in the engineering industry, and in no way reflect our beliefs or attitudes towards historical events or peoples. The terms are purely technical and must not carry any implications beyond their technical meanings.

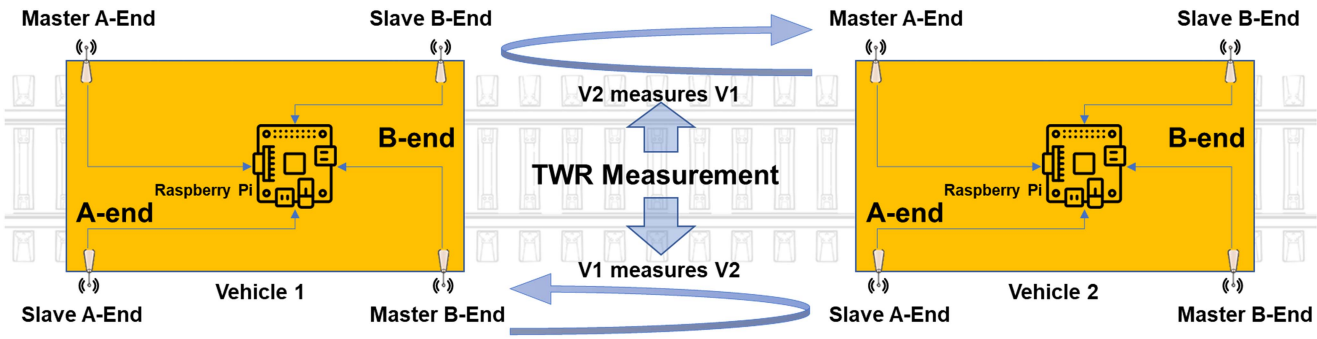

Fig. 2. Components and system layout of the UWB V2V ranging implementation for two example vehicles. The individual position of the devices relative to the vehicle is illustrated at each corner.

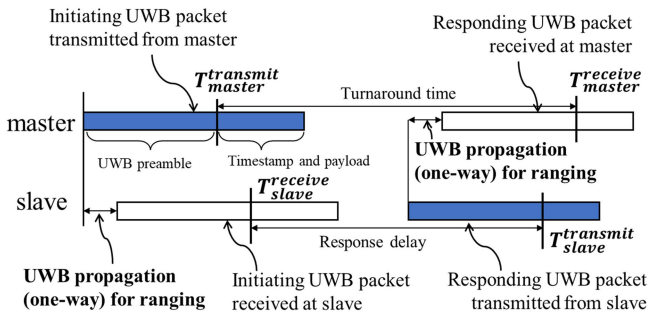

Fig. 3. UWB RTD distance ranging using the TWR algorithm. Packet abstraction shown here illustrates the UWB propagation delay used for ranging distance calculation.

device received packets from the slave device, and so forth. c denotes the speed of light as the UWB packet propagates. The process of the TWR algorithm and timestamp notations of (1) are illustrated in Fig. 3 (adapted from [44]).

During the TWR measurements, the master and slave devices are also configured to exchange application-specific data (called *Informative Position*) for onboard computers to process device-to-device distances into V2V distances. This component is designed to offset vehicle dimensions and maintain fine V2V ranging accuracy when vehicles get close. Accuracy supported by this function is very effective for collision avoidance amid accidents, risk control for close-call movements, and operation scenarios such as vehicle aggregation, grouping, and train consist assembly.

DWM1001-DEV UWB-IR transceiver modules by Decawave (Qorvo) are chosen in this study. They can be versatilely deployed as master mode or slave mode with our firmware. Raspberry Pi 3B+ serves as the onboard computer to provide power supply and host data processing services.

A. Data Engineering

Inside Decawave's original TWR-based UWB positioning system (DRTLS) [45], a mobile UWB tag infers its coordinates from two sets of input: 1). TWR ranging measurements with fixed UWB anchors 2). Coordinates of UWB anchors piggybacked by the UWB TWR messages. Our V2V ranging design preserved this original DRLTS networking protocol, but converted the UWB tag into master, and the UWB anchor into slave, with additional data modification described as follows.

DRTLS originally assigned 4 bytes for each Cartesian coordinate dimension (X, Y, Z) of UWB anchors in their TWR response to tags. This enables a 12-byte programmable datafield for each slave device to respond to its polling master. With strict frugality on the 12-byte budget, we repurposed this datafield to accommodate extra variables by balancing the precision and the value range for each field. In sum:

- Our design replaced the original absolute device coordination system with a new one relative to vehicle.
- Another three application variables have been fit in.
- Three bytes are spared for future extensibilities.

This application-specific data design is called *Informative Position*, covering the following variable definitions for both master and slave devices:

- Relative mounting position (Fig. 4, bottom):
  - Modified X-axis position:
    Longitudinal distance to the nearest vehicle coupler.
  - Modified Y-axis position:
    Lateral offset against the rail track centerline.
  - Modified Z-axis position:
    Vertical elevation towards the top of the rail head.
- Device mounting side ("A" or "B" end) of the vehicle.
- Vehicle length.
- Vehicle identifier (ID).

The byte allocation plan is elaborated in Table II and Fig. 4 (top). To encode the field measurements of *Informative Positions* for each device, we designed an Android application to flash different modes with their respective *Informative Position* data into UWB devices using Bluetooth.

B. Networking and V2V Ranging Algorithms

Before serving V2V ranging functions, slave devices must establish an ad-hoc UWB TWR ranging network to prepare synchronized clocks for the master device to poll. Reachable slave devices constantly maintain and adapt the ad-hoc UWB network as vehicles move. A ranging cycle can only be completed when the slave devices maintain a fresh network. If the network gets stale and the slave device loses its seat, it switches back to network initialization mode until its seat is reclaimed.

In one ranging cycle, a master device broadcasts a request and receives the customized UWB TWR response data from each visible slave device. A master device of vehicle i calculates the V2V distance $\delta d_{i,j}$ (more specifically, coupler-to-coupler

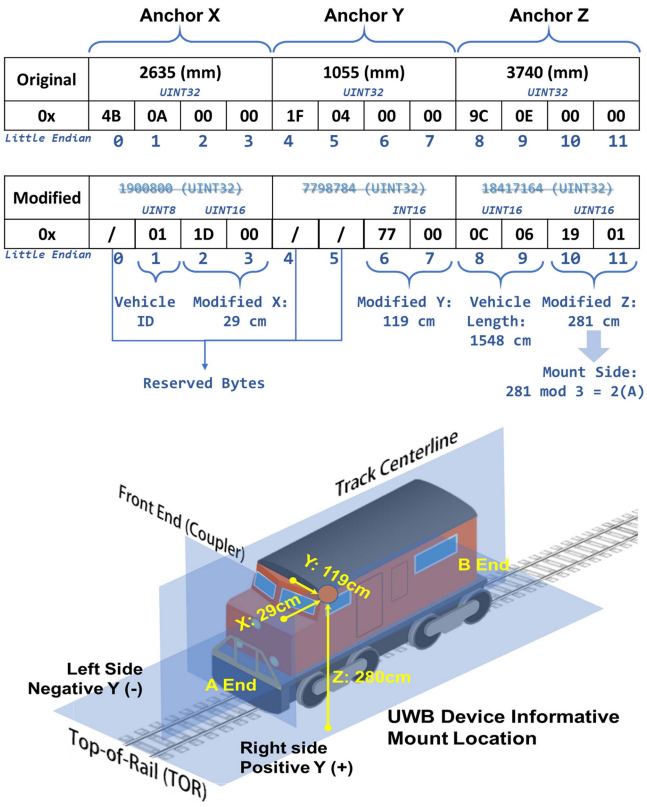

Fig. 4. Visualized byte customization in *informative position* compared to the original design (top) with sample values; the illustration of the sample device installation and axes definition relative to the rail vehicle (bottom).

TABLE II
INFORMATIVE POSITION DATA CATEGORIES AND BYTE ALLOCATION

Data Categories	Byte Allocation	Data Range/Unit/Type
Modified X-axis value x_{slave}, x_{master}	Byte 2 and 3 (little-endian)	0 – 65535 cm Unsigned INT16
Modified Y-axis value* y_{slave}, y_{master}	Byte 6 and 7 (little-endian)	-32768 – 32767 cm Signed INT16*
Modified Z-axis value z_{slave}, z_{master}	Byte 10 and 11 (little-endian)	0 – 65535 cm Unsigned INT16
Vehicle Length l_i	Byte 8 and 9 (little-endian)	0 – 65535 cm Unsigned INT16
Vehicle ID i	Byte 1	0 – 255 Unsigned INT8
Mounting End/Side s_{slave}, s_{master}	Z-value mod 3	2: "A", 1: "B", 0: N/A

* For modified Y-axis values, 0 represents track centerline.
Y-value signs (+/-): facing the vehicle from the track centerline:
- Negative value denotes right side; Positive value denotes left side.

distance) from a slave device of the adjacent vehicle j by:

$$\delta d_{i,j} = \sqrt{d_{uwb}^2 - y_{diff}^2 - z_{diff}^2} - x_{diff} \tag{2}$$

where d_{uwb} denotes the direct UWB TWR distance from the master device to the slave device; x_{diff}, y_{diff}, and z_{diff} denote the axis offsets of *Informative Position* along the corresponding dimensions.

Between two adjacent vehicles, there are four practical ranging scenarios to be considered, as illustrated in Fig. 5. For each scenario, dimensional offsets are calculated differently. In Fig. 5, *Informative Position* values of the devices' axes are denoted accordingly, such as $x^i_{master_A}$, which represents the X-axis *Informative Position* value for the "A" End master device on vehicle i. The other notations can be inferred correspondingly.

By design, any pair of master/slave devices among the four scenarios can simultaneously generate the same V2V/coupler-to-coupler distance. These four scenarios complement each other to support system redundancy. Noticeably, from V_i's perspective, *Scenario #1* represents the only device pair with the best line-of-sight (LOS) condition to V_j, which is considered the main pair. The other pairs are designated as auxiliary pairs. One rail vehicle can take either selective pairs or all the pairs to aggregate the V2V ranging results.

Since appliances on a vehicle may block the direct LOS radio path for auxiliary pairs, these V2V ranging results might not be as reliable as those of the main pair due to UWB's sensitivity to non-line-of-sight (NLOS) conditions. Therefore, results from both the main pair and all the aggregated pairs will be analyzed in the field-testing.

The original DRTLS system's time-division multiple access (TDMA) protocol supports an update rate up to 10 Hz for tag's positioning. Theoretically, the aggregated update rate can reach 40 Hz between two vehicles. The pseudocodes of networking and ranging algorithms for both slave and master devices are elaborated in Algorithm 1 and Algorithm 2. Their interactions are illustrated in Fig. 6 with a block diagram.

In the algorithm pseudocodes, $seat\_id$ denotes a volatile/ad-hoc ID of slave devices to form the UWB TWR network. $seat\_id$ must be unanimously agreed by all slave devices to start serving masters. $seat\_map$ denotes the set of key-value pairs that maps $seat\_id$ with mac_addr for all slave devices. mac_addr denotes the device media access control address, which is persistent and non-volatile. $info\_pos$ denotes *Informative Position* defined in this study. clk_epoch denotes the local clock of devices. It is the target variable for clock synchronization. $master\_twr\_init$ denotes the TWR initialization requests from master to slave devices. $Rx/Tx\_timestamps$ denotes the timestamps on slave devices for receiving a TWR request from and responding the TWR request to a master device. $v2v\_dist$ denotes the concerned vehicle-to-vehicle ranging distance reported by our system.

C. Vehicle End/Side Detection

In safe railroad operations, it is critical to gain awareness of an on-track vehicle's orientation for V2V distance ranging. In our system, the closest end of an adjacent vehicle can be inferred by the host vehicle using the ranging data received from multiple pairs of master/slave devices. Once the closest end of the adjacent vehicle is calculated by the host vehicle, the safety distance between the correct ends of both vehicles can be reliably

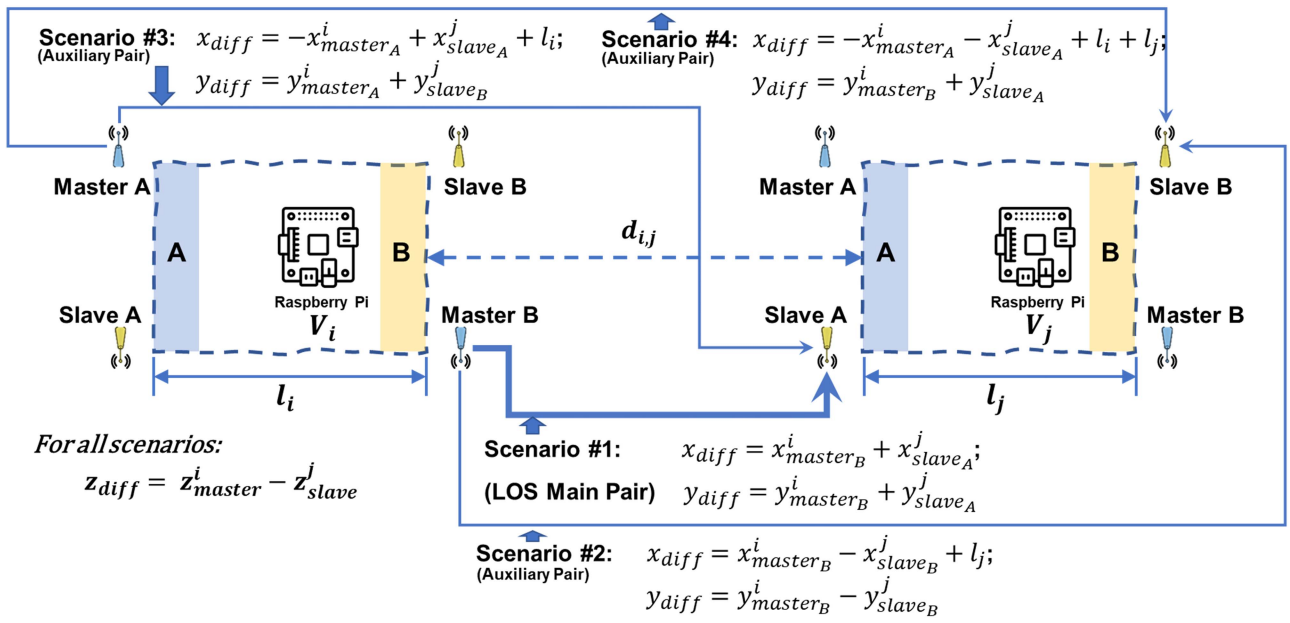

Fig. 5. Four V2V ranging scenarios and their axis offset calculations from V_i to V_j (ranging from V_j to V_i is not shown).

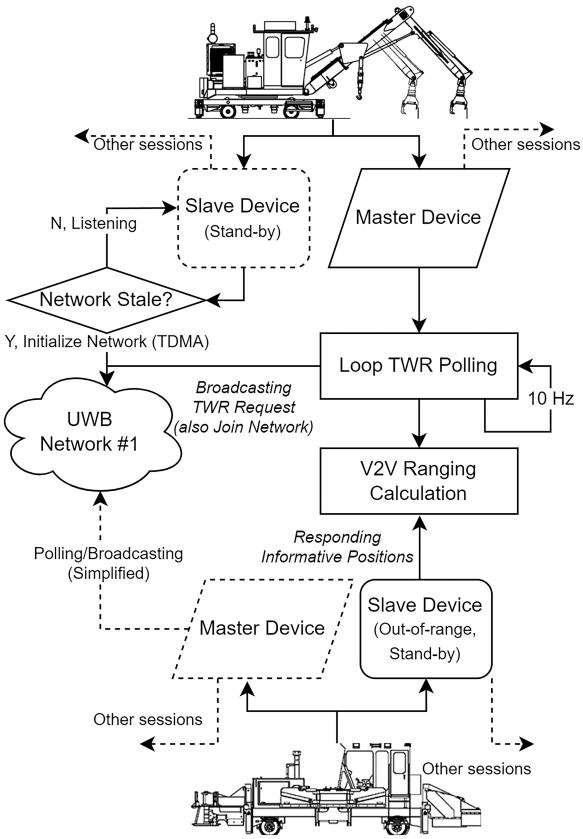

Fig. 6. Block diagram of vehicle/device interactions in V2V ranging system.

Algorithm 1: Slave Devices – UWB Cooperative V2V Ranging.

Attributes: seat_id, seat_map, mac_addr, info_pos, clk_epoch
Input: master_twr_init
Output: info_pos, clk_epoch, Rx/Tx_timestamps

Initialization (TDMA):

1. **Function** *TDMANetworking*(seat_id, seat_map, clk_epoch)
   /* recursive seat allocation & clock sync among slave devices */
2. **while** seat_id **NOT** unanimously agreed by reachable slaves **do**
3. receive seat_id requests and seat_map from neighbor slave devices
4. transmit seat_id requests and seat_map using ALOHA protocol
5. **if** packets collide **then**
6. randomized backoff, change seat_id, and **GOTO** step 5
7. seat_id, seat_map, clk_epoch ← *TDMANetworking*(seat_id, seat_map, clk_epoch)
8. **else**
9. lock seat_id, update seat_map, and synchronize clk_epoch
10. **return** seat_id, seat_map, clk_epoch
11. **end if**
12. **end while**

V2V ranging duty:

13. **while true**:
14. **if** receive master_twr_init packet **then**
15. transmit info_pos, mac_addr, clk_epoch, Rx/Tx_timestamps
16. **end if**
17. periodically send/check almanac among reachable slaves in TDMA network to determine network status
18. **if** network down (fresh→stale) **then**
19. **break** and **GOTO** step 1
20. **end if**
21. **end while**

processed from only one ranging pair of master/slave devices thereafter.

To infer the correct end (either "A" or "B") of rail vehicles under the byte budget, we compressed the modified Z-axis value to carry the additional information of the device's mounting end. The implementation of encoding and decoding algorithms is explained below:

$$z_{encode} := \underset{i \in Z^*}{\operatorname{argmin}} \left(3 \times \left[\frac{i}{3} \right] + S_{meas.} - z_{meas.} \right), \quad z_{meas.} \in Z^*, S_{meas.} \in \{0, 1, 2\} \tag{3}$$

Algorithm 2: Master Devices – UWB Cooperative V2V Rnging.

Attributes: mac_addr, info_pos, clk_epoch
Input: info_pos, clk_epoch, Rx/Tx_timestamps (by slave device)
Output: v2v_dist

V2V ranging duty:

1. **while true**:
2. periodically broadcast master_twr_init packet (0.1 second interval)
3. **for** {info_pos, clk_epoch, Rx/Tx_timestamps} ∈ responses **do**
4. calculate v2v_dist ← δd from expression (1) and expression (2)
5. **end for**
6. **end while**

$$S_{decode} = z_{encode} \mod 3,\ z_{encode} \in Z^* \tag{4}$$

where z_{encode} denotes the encoded Z-axis value in centimeters. $z_{meas.}$ denotes the field-surveyed Z-axis *Informative Position* value of the device. $S_{meas.}$ denotes the factual mounting end of the device on the vehicle. S_{decode} denotes the mounting end of the device inferred by the UWB ranging system on the other vehicle. S variable has three legal values: 0, 1, and 2, in which 2 maps to "A" end, 1 maps to "B" end, and 0 represents invalid values. This compression encoding algorithm only introduces less than 2 cm of error along Z-axis. Such error constitutes an even smaller projective error along X-axis, which is the most concerned dimension in this study.

The holistic design of *Informative Position* and its associated algorithms empower the collaboration of auxiliary pairs and the main pair between two vehicles. With the help of the customized application data (*Vehicle ID*, *Vehicle Length*, and *Device Mounting Side*), vehicles mutually determine their respective ranging scenarios as illustrated in Fig. 5, and conduct the distance calculation to convert raw UWB inputs into accurate V2V ranging distances. Employing the redundancy from multiple input pairs and the confined motion freedom of on-track rail vehicles, the V2V ranging results can create an enriched perception to further accommodate track curvature, fleet scalability, and track distinction in rail yards.

V. Field-Testing Design

In collaboration with Norfolk Southern Railway, a major freight railroad company in the United States, we conducted a field-testing to evaluate the technological credibility of UWB, the design effectiveness, and the overall system performance. A section of straight, flat, and open-air standard-gauge rail track in Selinsgrove, Pennsylvania, USA was chosen as the testing site. Two self-propelled MOW rail vehicles: track tamper (V1) and ballast regulator (V2) were drafted to carry out the test. Their max speeds top at 30 mph (48 km/h).

In the field-testing, we focused on benchmarking the performance metrics for the designed system, including ranging accuracy, max ranging distances, speed responsiveness, update rate, and overall effectiveness of *Informative Position* data. We also intended to verify the system's capability to improve drivers' distance awareness, and to explore if a realistic rail environment can cause significant impacts on UWB's propagation and jeopardize its communication.

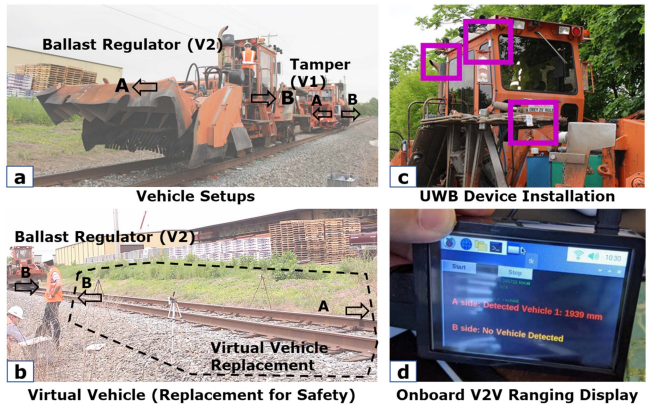

Fig. 7. System deployment on field-testing vehicles and onboard display: (a) Testing vehicles. (b) Virtual vehicle setup. (c) UWB device onboard installation. (d) Onboard V2V ranging display.

To provide desired LOS propagation conditions, UWB master and slave devices were installed around the peripheral of vehicles' cabs with decent elevation, configured with accurate *Informative Position* from field surveys by millimeter-level laser range finders. The setup, layout, site conditions, and onboard ranging display of the field-testing are shown in Fig. 7.

Two categories of test, *Static Test* and *Moving Test*, were carried out in the field-testing. In *Static Test*, both vehicles sat still when the V2V ranging system collected data against each other. Laser range finders were used to measure the reference distance among vehicles. We positioned V2 at 13 different locations to collect the V2V ranging data against V1. For each location, 2 minutes of V2V ranging data were continuously collected.

In *Moving Test*, we operated the moving vehicle (V2) at varying speeds against the static vehicle (V1), intended to test the speed responsiveness when the vehicles move. Seven (7) tests were conducted at varying speeds in both directions of the track. For safety reasons, the physical static vehicle (V1) was replaced by a virtual vehicle at higher testing speeds (V3, illustrated in Fig. 7(b)). The virtual vehicle consists of 4 UWB devices mounted on tripods, positioned outside the track loading gauge, simulating the contour of a dummy vehicle. Five (5) additional tests were conducted using this virtual setup. The conducted tests and setups are summarized in Table III.

To acquire the instant location and speed of a vehicle when it moves, we designed an ad-hoc camera-based onboard location reference system, illustrated in Fig. 8. During vehicle movements, the reference system uses an onboard downward-facing camera to capture pre-surveyed ground markers with a synchronized clock, at a rate of 15 FPS. The ground markers were installed along the testing track with a fixed separation of 4 ft (1.21 m). In the field-testing, we covered a 150 ft (45.7 m) track section with markers for vehicle movement references.

Intermediate reference locations between adjacent markers are interpolated by timestamps. Same as the onboard UWB devices, the *Informative Position* of the camera was also surveyed and recorded. We developed a simple machine vision algorithm to infer the camera's positions relative to the markers from the video frames. Subsequently, the surveyed *Informative Position* of the camera is used to calculate the instant location and speed of

TABLE III
FIELD-TESTING SETUP AND CONFIGURATION

Static Test	Static Test Setup	Moving Test	Moving Test Setup	Is Virtual	Moving Test Speed (Nominal)
#1	6.002m	#1	Separating	N	Walking Speed
#2	7.8m	#2	Separating	N	3mph
#3	9.541m	#3	Separating	N	5mph
#4	11.278m	#4	Approaching	N	4mph
#5	13.094m	#5	Separating	N	12mph
#6	14.973m	#6	Separating	N	12mph
#7	17.247m	#7	Approaching	N	5mph
#8	18.986m	#8	Separating	Y	Varying, 6mph max
#9	21.736m	#9	Separating	Y	10mph
#10	24.651m	#10	Separating	Y	20mph
#11	27.381m	#11	Separating	Y	10mph
#12	29.877m	#12	Separating	Y	1mph
#13	32.499m	/	/	/	/

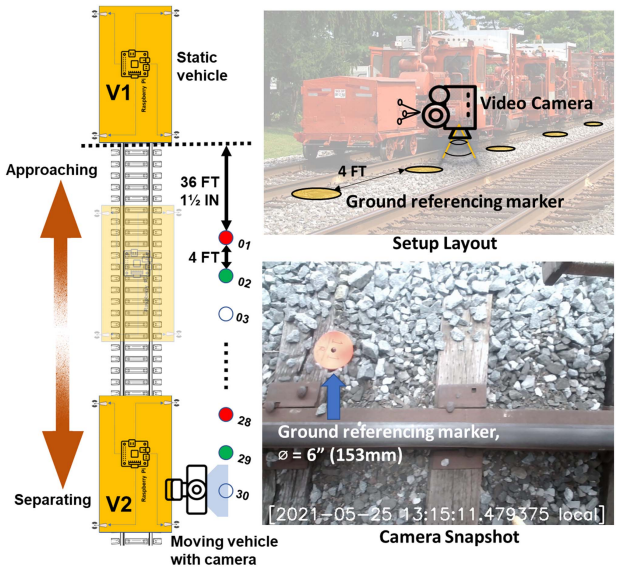

Fig. 8. Ground location reference system for moving vehicle. Background image courtesy of American-Rails.com.

the moving vehicle, and hence the V2V distance to be compared with results from the UWB ranging system.

VI. TEST RESULT ANALYSES AND SIMULATION EVALUATION

A. Ranging Accuracy and Functional Integrity

We evaluate the V2V ranging accuracy from the following field-testing results:

- The V2V ranging accuracy at the application-level.
- The effectiveness of the correction function to convert raw device-to-device distance to V2V ranging distance.

The ranging error is considered as the difference between the ranging measurements and the ground references. The ground references come from either laser range finders in *Static Tests*, or camera frame interpolations in *Moving Tests*. The accuracy summary from our field-testing is presented in Table IV.

TABLE IV
ACCURACY SUMMARY, CATEGORIZED BY VEHICLES AND DEVICE PAIRS

Tests	Average Error (mm)		Standard Deviation (STD, mm)	
	Main Pair	All Pairs	Main Pair	All Pairs
	Static Vehicle (Rail Tamper, V1)			
Static (13)	-18.3	-13.4	96.1	165.1
Moving (7)	-277.7	-245.4	150.1	177.4
	Moving Vehicle (Ballast Regulator, V2)			
Static (13)	-89.0	-113.4	92.9	118.4
Moving (7)	-401.6	-390.3	155.4	156.0

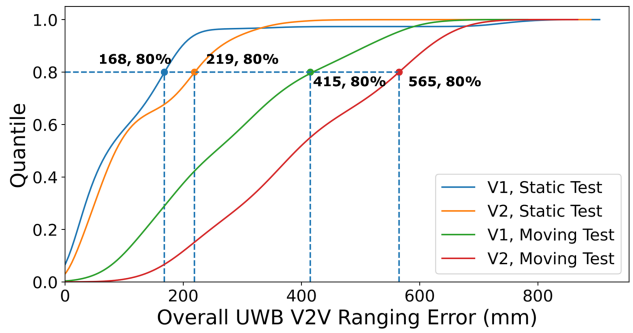

Fig. 9. Cumulative distribution function (CDF) of the difference between the V2V distance measured by our UWB system and the ground references.

In 13 *Static Tests*, the average V2V ranging error on both vehicles rendered less than 10 cm for both the main and aggregated pairs (all 4 pairs). The error standard deviation (STD) was controlled at 20 cm, which is considered satisfying for our design scope. In 7 *Moving Tests*, the average error and error STD went up to the 40 cm-level and 250 cm-level, respectively. The overall ranging error of the system is illustrated in Fig. 9 in the form of CDF curves: as for the 80%-quantile error, V1 and V2 were measured with 16.8 cm and 21.9 cm in *Static Tests*. In *Moving Tests*, the numbers increased to 41.5 cm and 56.5 cm, respectively.

In this case study, the effectiveness of the *Informative Position* ranging distance correction is shown in Fig. 11 using *Moving Test* results, as our system converted the raw UWB device-to-device ranging distances to the V2V ranging distances. Before the system correction, the raw UWB ranging error was at 250 cm-level. The final result of the V2V ranging error was confined within 80 cm after the correction.

Noticeably, we observed a quasi-linear relationship between the ranging error and the factual distance, where the error became larger when two vehicles got closer. The system correction also reduced such effect by flattening the linear slope from -0.0178 to -0.0163, an improvement of 8.4%. These observations successfully validated the system design effectiveness, whose functions aim to mitigate the accuracy impacts of vehicle dimensions at variable distances.

Compared to the *Static Test*, *Moving Test* presented both higher error and error STD. The causes include vehicle vibrations, manual survey biases, and limited accuracy for ground location referencing (low camera FPS and discrepancies in marker

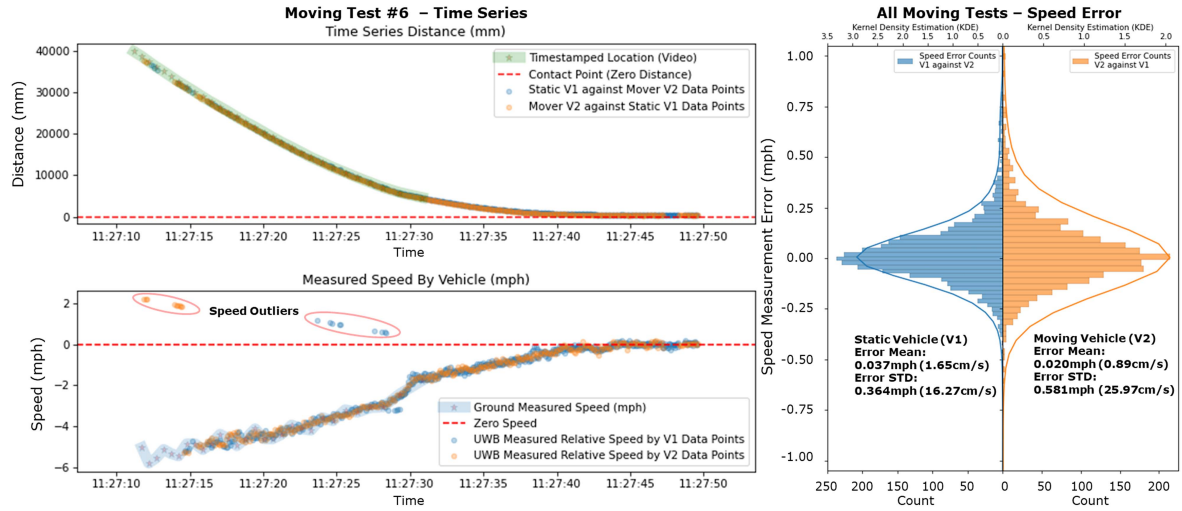

Fig. 10. Speed measurements example (*moving test #6*) and aggregated speed error distribution for all *moving tests*.

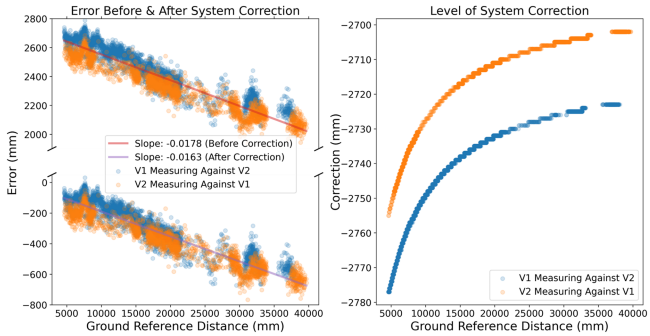

Fig. 11. *Moving test* ranging error (bias) on both vehicles, before (upper left) and after (bottom left) cooperative system correction (right).

placement). Specifically, in terms of credibility, we acknowledge that the marker-based ground location reference system in *Moving Test* is not on par with the laser range finders used in *Static Test*. Thus, we argue that although the error appeared to be higher in *Moving Test*, it might result from the ground reference, instead of the system performance. Therefore, we still deem the downgraded average error and error STD acceptable.

B. Max Ranging Distance

The max ranging distance between vehicles is constrained by the -41.3 dBm/MHz UWB transmitting power limits [46]. In the test results, the practical max V2V ranging distance achieved 32.5 m in *Static Test* (*Static Test #13*, shown in Fig. 15), and 40 m in *Moving Test* (max X-value shown in Fig. 13). Meanwhile, Decawave, the vendor of UWB transceivers used in this research, has claimed 300 m max range between devices [47]. The gap between the claimed distance and our field-testing data should be due to the following two factors:

- The uncontrollable radio frequency (RF) conditions in the testing site might prematurely dampen the UWB signal by other noises. The UWB propagation characteristics in the testing site may not be as favorable as the vendor's calibration.
- Our system adopted the native TDMA networking protocol by Decawave. However, the specific TDMA protocol is optimized for positioning services at fixed sites. It may impose constraints on the max range in our modified mobile system.

To unleash the max potentials of UWB-IR technology for the selected V2V ranging use case, we argue that improvements in our implementations can be made using better antennas and higher transmitting power to achieve longer range, and a purpose-built networking protocol should resolve unnecessary radio collisions, and extend the max range.

C. Relative Speed Responsiveness

Awareness of relative speed is significant for the safety of self-propelled rail vehicles, helping operators to brake accordingly. In *Moving Test*, the instant relative speeds between two vehicles were measured by the time differential of V2V ranging distances. Fig. 10 (left) shows an example (*Moving Test #6*) of the UWB-measured V2V ranging distance and instant speed data by ground reference. In the example, V2 approached V1 at 6 mph (2.7 m/s) from 40+ meters away. The UWB speed measurements in the V2V ranging system strictly followed the ground-referred data. The errors present a normal distribution with close-to-zero means and minimal STD, as shown in Fig. 10 (right). Therefore, the relative speed measurement between vehicles in our implementation is considered precise and accurate.

D. Multipath Effect

For individual master/slave device pairs, the V2V ranging results strictly followed normal distribution. The multipath effect of UWB can be observed from the normal distribution data clusters generated by auxiliary pairs, where the multipath delay of UWB leads to higher ranging distances, and contributes to higher average error in the ranging results (Fig. 12). In this example, ranging results of V1 from *Static Test #5* recorded 2 additional channel paths for the master/slave device pair of 9B0F/1912 (i.e., *Scenario #3*, Fig. 5). As compared to the direct

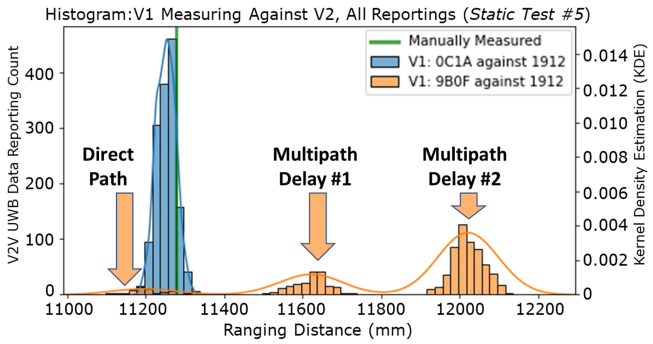

Fig. 12. Data sample of *static test #5* showing the multipath effect: Receiver vehicle: V1.

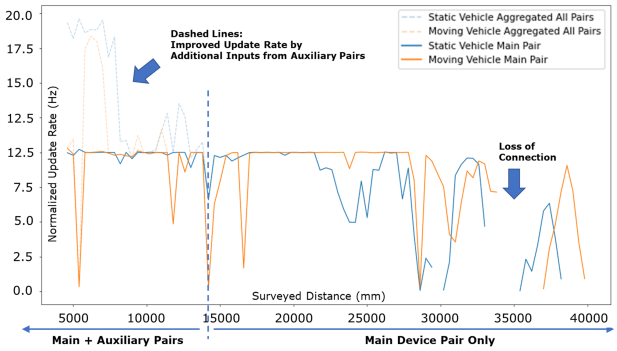

Fig. 13. *Moving test*: Normalized update rate (categorized by pairs) vs. surveyed distances.

path (0C1A/1912), the additional channel paths of 9B0F/1912 are 40 cm-longer and 80 cm-longer respectively.

With the conservative safety views, the V2V ranging system can always filter out ranging results from larger-value clusters to choose the shortest distances from the direct path. Downstream V2V ranging data consumers always get the minimum distance that this system can report. Such a naive approach can be deemed valid when the system serves a safety-critical function such as collision avoidance.

E. System Capacity, Redundancy, and Stability

UWB communications always desire LOS conditions. Our seat-based decentralized networking protocol is also sensitive to packet collisions and transceiver synchronization. Although the proposed system equips each vehicle with two sets of master and slave devices in favor of LOS and redundancy (Fig. 5), it is imperative to derive the capacity and capabilities under varied operational conditions and how these variables can converge. Therefore, we developed a full-scale replica in Gazebo-ROS[2] to cover the unvisited scenarios from field-testing.

The simulation intends to explore the performance boundary and functional stability of our V2V ranging system considering the following variables: relative vehicle speed, max UWB range, ranging update rate, and collision avoidance effectiveness. The simulation is built as follows:

[2]https://github.com/hegxiten/uwb_v2v_ros_sim

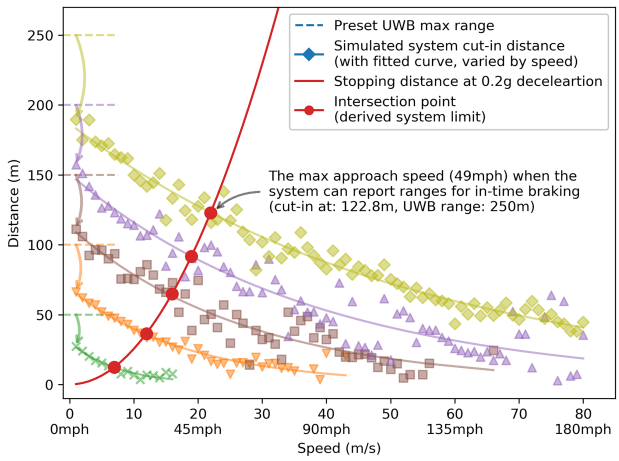

Fig. 14. Simulated results of effective V2V ranging cut-in distance at varied approach speeds. A simple assumed stopping distance (at 0.2g deceleration) outlines the effective area when used as a collision avoidance system (CAS).

- A complete replica of TDMA networking algorithms.
- Two simulated vehicles, one moving straight towards the other at varied speeds (1 m/s to 80 m/s, 80 steps).
- Simulated packet loss and collision probability model for both networking stages and master-slave interaction stages (a linear inverse model over node spacings).
- Real representations of UWB network seat cap, max UWB ranges (50 m to 250 m, 5 steps), and rates of handshaking and broadcasting (0.2-sec stale threshold for synchronization, 10 Hz master base reporting rate).
- Define effective V2V ranging cut-in distance as the momentary distance when both vehicles receive at least 5 Hz of V2V ranging reports during approach. Subsequent V2V ranging rates ramp up to 40 Hz.

With 15 epochs on each simulation step, the theoretical limits of the system have been derived as Figs. 14 and 16, explained as follows:

- At 50 m max UWB range, the system can support V2V ranging up to 37.5 mph relative speed (before the networking period exhausts the time).
- At 50 m max UWB range, if stopping distance is considered as a constraint, vehicles should not operate at more than 6 m/s (14 mph) relative speed free of collision risk.
- Results simulated under 50 m max UWB range generally conform with our field-testing observations, proving the suitability of the chosen use case (self-propelled rail vehicles at medium-to-slow operating speed).
- The gap between the system's cut-in distance and max UWB range (annotated by arrows) reflects the time overhead for individual UWB transceivers to establish the decentralized network for ranging support. Higher speed and lower UWB range contribute to higher costs in performance, i.e., the networking overhead.
- The region above the intersections between stopping distance curves and fitted distance-speed curves indicates the effective zone of our V2V ranging system to support the CAS function. With a more reliable stopping distance model, its applicability can also scale up.

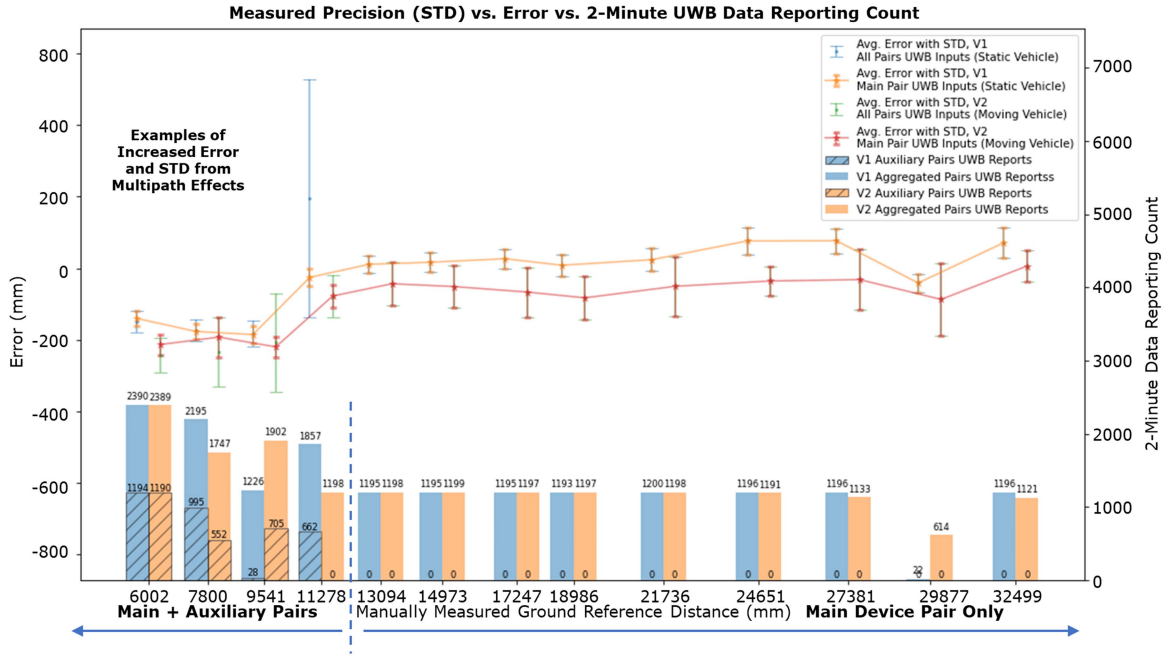

Fig. 15. *Static test*: Overview of UWB input counts, categorized by pairs.

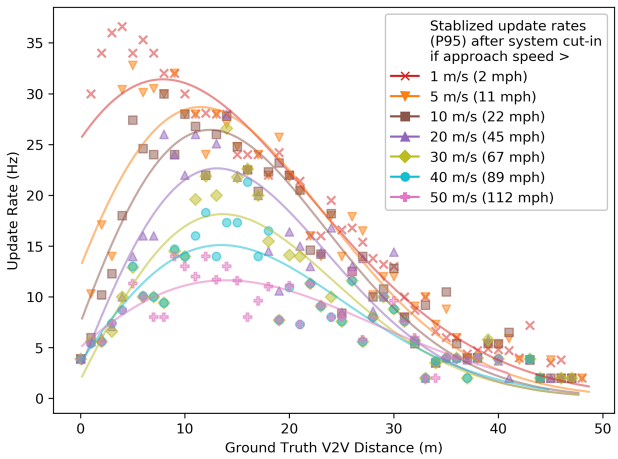

Fig. 16. Aggregated simulated results of stablized update rates (at 95th percentile) when the max UWB range is preset as 50 m (close to field observations). The lowered aggregated update rates with higher approach speeds or longer V2V distances effectively reflect the observed connection drops in individual runs at field-testing.

Fig. 16 shows the cap of instantaneous update rates (95th percentile) for the system at varied speeds under the preset 50-m max UWB range. Using the update rate as the evaluation metric, it indicates the best theoretical performance of the system converged at varied speeds and ranging distances after enough simulation runs.

VII. Conclusion and Discussions

In this study, we chose UWB-IR technology to design and assess a communication-based cooperative V2V ranging system for self-propelled rail vehicles. The advantages of UWB technology in ranging and the application uniqueness of self-propelled rail vehicles (e.g., the dimensions, motion patterns, and rail-specific operational roles) jointly inspired the case study and fused the fitness-to-purpose of the system. The design evolved from a real-time UWB positioning system by Decawave, flavored by the particular application patterns and algorithm design. Its effectiveness has been validated in the field-testing, and its stability has been derived from Gazebo-ROS simulation. Specifically, the following system characteristics have been benchmarked:

- Ranging accuracy (centimeter-level average errors, with 20 cm-level error STD).
- Update rate and redundancy (10 Hz in the specification; reached 20 Hz by auxiliary redundancy).
- Speed responsiveness (0.05 mph-level average error, with 0.5 mph-level error STD).
- Theoretical max ranging distance, system effectiveness by relative speeds, and conditional limits under stopping distance.

The 40 m max ranging distance observed in field-testing may restrict the system's application scale. In practice, there are scenarios when self-propelled on-track rail vehicles move with a separation of more than 40 m. As the simulation result shows, broader application scenarios require a longer range of UWB communication or shorter UWB protocol networking time overhead. The improvement options include directional antennas, better device installation plans, higher legalized transmission power, and fine-tuned networking algorithms.

In addition, complicated operational scenarios should be considered in future testing and validation work. The topics include but are not limited to:

- Variety of track geometry:
  A longer-distance rail-based V2V ranging system should consider curvatures and gradients to rectify safety-critical

measurements. The consideration to accommodate track geometry resembles the concepts of *Informative Position* design to account for vehicle dimensions.

- Fleet-level scalability:
  Due to the restricted resources, our case study has only employed two vehicles. The scalability of the system could not be tested at a mass level. With the simulation platform, we plan to conduct future research to answer how many vehicles can range simultaneously without overloading the network, and we also plan to keep improving the networking algorithm iteratively under scaled contexts.
- Complexity of rail yard operations:
  The current system is able to distinguish between "A" and "B" end of an adjacent vehicle. This feature should acclimate to multi-track scenarios such as rail yard with parallel tracks, switches, and complex route topologies.

During field-testing, scenarios of occasional missing data have been observed. Missing data indicated UWB connection drops, when the master devices could not receive V2V ranging responses from any slave devices. We noticed the data loss also happened before the system reached the observed max ranging distances. We presume that the major cause of such data loss is not the limit of UWB transmission power. Rather, the TDMA networking protocol might not have well-sustained the dynamics in these test cases. The connection drop may come from the contention-prone mechanism where slaves establish the network to sync clocks and serve masters. In our simulation, the simplified packet loss probability model could also reproduce similar behaviors occasionally. The overall behaviors are reflected in the simulated update rates over distances (Fig. 16), and the distribution is highly model-dependent.

Envisioning future analyses and mitigations on the connection drop, we propose the following methods for preliminary system modeling and simulation adaptation. For instance, within the max theoretical peer-to-peer UWB ranges (such as 300 m declared by the manufacturer [47]), optimizing the stability of the ad-hoc UWB network established between vehicles shall have the following form of objective:

$$\min\ P_{drop} = F\left(\delta d_{i,j}, \delta v_{i,j}, n_{slave},\ n_{master}, m_{slave},\ m_{master}, \Delta t_{init}, G_t,\ p\right) \tag{5}$$

where P_{drop} denotes the variable probability of connection drop between vehicle i and j. $\delta d_{i,j}$ and $\delta v_{i,j}$ denote the factual distance and the factual relative speed between vehicle i and j. n denotes the number of UWB nodes joined in the network. m denotes the number of UWB nodes trying to join the network. Δt_{init} is the configured polling rate on masters. G_t abstracts the current spatial topology for all devices. p represents the basic connection drop probability of UWB communication in simple peer-to-peer conditions. Typically:

- $\delta d_{i,j}$ is constrained by vehicle practical distances.
- $\delta v_{i,j}$ is constrained by vehicle practical speeds.
- Δt_{init} is configured by the system, up to 0.1 sec (10 Hz).
- G_t is constrained by the track geometry and past states.
- p can be acquired from lab testing.

$n_{slave},\ n_{master}, m_{slave},\ m_{master}$ could jointly be acquired from a finite-state machine $M = (S,\ s_0,\ s_t, G_t, m_t,\ n_t,\ f)$ based on historical states and current observations, where S represents the set of networking states formed by UWB devices and vehicles, depending on the exhaustive enumeration of ranging status and network freshness. s_0 is the initial state describing the items above. $s_t,\ m_t, n_t$ describe the momentary state t as the input to the current optimization objectives. f is the state transition function pending detailed modeling. In general, although it leaves an open-ended question for now, the foregoing discussions should guide the course of future follow-up studies and expect vivid research efforts.

In future work, we will focus on the chosen TDMA networking algorithms and protocol design to investigate the causes of connection degradation following the guidelines above. Further computer modeling and simulation work will be carried out based on the proposed optimization methodology. Trimming the UWB networking protocol to better fit the cooperative, distributed characteristics in the V2V ranging applications should presumably resolve connection issues and improve the general performance. To further promote the system, sensor fusion concepts will also be considered to maximize the applicability and generality of the development in both academia and industry.

ACKNOWLEDGMENT

This study was supported by a research grant from the Federal Railroad Administration (FRA) of the U.S. Department of Transportation (DOT), grant ID: 693JJ619C000013. The authors thank our collaborator railroad company for the field-testing support and FRA for the funding support. The views and opinions expressed herein are those of the authors and do not necessarily state or reflect the U.S. DOT or the FRA, and shall not be used for advertising or product endorsement purposes.

REFERENCES

[1] F. Maire and A. Bigdeli, "Obstacle-free range determination for rail track maintenance vehicles," in *Proc. 11th Int. Conf. Control Automat. Robot. Vis.*, 2010, pp. 2172–2178, doi: 10.1109/ICARCV.2010.5707923.

[2] F. Maire, "Vision based anti-collision system for rail track maintenance vehicles," in *Proc. IEEE Conf. Adv. Video Signal Based Surveill.*, 2007, pp. 170–175, doi: 10.1109/AVSS.2007.4425305.

[3] U.S. Department of Energy, "ARPA-E oPEN 2021 project descriptions," 2021. Accessed: Feb. 14, 2022. [Online]. Available: https://arpa-e.energy.gov/document/open-2021-project-descriptions

[4] Z. Zeng, S. Liu, W. Wang, and L. Wang, "Infrastructure-free indoor pedestrian tracking based on foot mounted UWB/IMU sensor fusion," in *Proc. 11th Int. Conf. Signal Process. Commun. Syst.*, 2017, pp. 1–7, doi: 10.1109/ICSPCS.2017.8270492.

[5] J. Zhu and S. S. Kia, "A SPIN-based dynamic TDMA communication for a UWB-based infrastructure-free cooperative navigation," *IEEE Sensors Lett.*, vol. 4, no. 7, pp. 1–4, Jul. 2020, doi: 10.1109/LSENS.2020.3004890.

[6] FRA Office of Safety Analysis, "FRA accident data as reported by railroads," 2021. Accessed: Mar. 3, 2022. [Online]. Available: https://safetydata.fra.dot.gov/officeofsafety/publicsite/on_the_fly_download.aspx

[7] U.S. DOT FRA, "Office of safety analysis, 'train accident cause codes," 2021. Accessed: Mar. 04, 2022. [Online]. Available: https://safetydata.fra.dot.gov/OfficeofSafety/publicsite/downloads/appendixC-TrainaccidentCauseCodes.aspx?State=0

[8] J. Marais, J. Beugin, and M. Berbineau, "A survey of GNSS-based research and developments for the European railway signaling," *IEEE Trans. Intell. Transp. Syst.*, vol. 18, no. 10, pp. 2602–2618, Oct. 2017, doi: 10.1109/TITS.2017.2658179.

[9] L.-W. Chen and Y.-F. Ho, "Centimeter-grade metropolitan positioning for lane-level intelligent transportation systems based on the internet of vehicles," *IEEE Trans. Ind. Informat.*, vol. 15, no. 3, pp. 1474–1485, Mar. 2019, doi: 10.1109/TII.2018.2854901.

[10] M. N. Ahangar, Q. Z. Ahmed, F. A. Khan, and M. Hafeez, "A survey of autonomous vehicles: Enabling communication technologies and challenges," *Sensors*, vol. 21, no. 3, Jan. 2021, Art. no. 706, doi: 10.3390/s21030706.

[11] F. De Ponte Müller, "Survey on ranging sensors and cooperative techniques for relative positioning of vehicles," *Sensors*, vol. 17, no. 2, Feb. 2017, Art. no. 271, doi: 10.3390/s17020271.

[12] A. Acharya, S. Sadhu, and T. K. Ghoshal, "Train localization and parting detection using data fusion," *Transp. Res. Part C Emerg. Technol.*, vol. 19, no. 1, pp. 75–84, Feb. 2011, doi: 10.1016/j.trc.2010.03.010.

[13] X. Liu et al., "Cyber security risk management for connected railroads," Department of Transportation, Federal Railroad Administration, Washington, DC, USA, Tech. Rep. DOT/FRA/ORD-20/25, 2020.

[14] M. N. Cheptsov, S. I. Tsykhmistro, A. B. Boinik, and I. G. Bakhal, "Project near^2-network of European/Asian rail research capacities (signalling systems)," 2013. Accessed: Mar. 4, 2022. [Online]. Available: https://elibrary.ru/item.asp?id=27205580

[15] L. Yang, T. Mo, and H. Li, "Research on V2V communication based on peer to peer network," in *Proc. Int. Conf. Intell. Auton. Syst.*, 2018, pp. 105–110, doi: 10.1109/ICoIAS.2018.8494142.

[16] C. B. S. T. Molina, J. R. de Almeida, L. F. Vismari, R. I. R. González, J. K. Naufal, and J. Camargo, "Assuring fully autonomous vehicles safety by design: The autonomous vehicle control (AVC) module strategy," in *Proc. 47th Annu. IEEE/IFIP Int. Conf. Dependable Syst. Netw. Workshops*, 2017, pp. 16–21, doi: 10.1109/DSN-W.2017.14.

[17] H.-M. Cheng, C. Chou, and D. Song, "Vehicle-to-vehicle collaborative graph-based proprioceptive localization," *IEEE Robot. Automat. Lett.*, vol. 6, no. 2, pp. 990–997, Apr. 2021, doi: 10.1109/LRA.2021.3056032.

[18] Q. Guo et al., "An integrated UAV-borne lidar system for 3D habitat mapping in three forest ecosystems across China," *Int. J. Remote Sens.*, vol. 38, no. 8–10, pp. 2954–2972, May 2017, doi: 10.1080/01431161.2017.1285083.

[19] D. F. Pierrottet, G. Hines, B. Barnes, F. Amzajerdian, L. Petway, and J. M. Carson, "Navigation Doppler lidar integrated testing aboard autonomous rocket powered vehicles," in *Proc. AIAA Guid., Navigation, Control Conf.*, 2018, Art. no. 0614, doi: 10.2514/6.2018-0614.

[20] K. Cai, B. Wang, and C. X. Lu, "AutoPlace: Robust place recognition with single-chip automotive radar," in *Proc. Int. Conf. Robot. Automat.*, 2022, pp. 2222–2228.

[21] M. Shan, J. S. Berrio, S. Worrall, and E. Nebot, "Probabilistic egocentric motion correction of lidar point cloud and projection to camera images for moving platforms," in *Proc. IEEE 23rd Int. Conf. Intell. Transp. Syst.*, 2020, pp. 1–8, doi: 10.1109/ITSC45102.2020.9294601.

[22] W. Zhangyu, Y. Guizhen, W. Xinkai, L. Haoran, and L. Da, "A camera and LiDAR data fusion method for railway object detection," *IEEE Sensors J.*, vol. 21, no. 12, pp. 13442–13454, Jun. 2021, doi: 10.1109/JSEN.2021.3066714.

[23] S. Gupta, P. K. Rai, A. Kumar, P. K. Yalavarthy, and L. R. Cenkeramaddi, "Target classification by mmWave FMCW radars using machine learning on range-angle images," *IEEE Sensors J.*, vol. 21, no. 18, pp. 19993–20001, Sep. 2021, doi: 10.1109/JSEN.2021.3092583.

[24] Z. Wang, G. Yu, B. Zhou, P. Wang, and X. Wu, "A train positioning method based-on vision and millimeter-wave radar data fusion," *IEEE Trans. Intell. Transp. Syst.*, vol. 23, no. 5, pp. 4603–4613, May 2022, doi: 10.1109/TITS.2020.3046497.

[25] K. Uchiyama and A. Kajiwara, "Vehicle location estimation based on 79 GHz UWB radar employing road objects," in *Proc. Int. Conf. Electromagn. Adv. Appl.*, 2016, pp. 720–723, doi: 10.1109/ICEAA.2016.7731500.

[26] K. Uchiyama, T. Motomura, and A. Kajiwara, "A study on self-vehicle location estimation employing 79 GHz UWB radar," in *Proc. IEEE Sensors Appl. Symp.*, 2018, pp. 1–5, doi: 10.1109/SAS.2018.8336785.

[27] S. Sivaraman and M. M. Trivedi, "Looking at vehicles on the road: A survey of vision-based vehicle detection, tracking, and behavior analysis," *IEEE Trans. Intell. Transp. Syst.*, vol. 14, no. 4, pp. 1773–1795, Dec. 2013, doi: 10.1109/TITS.2013.2266661.

[28] Y. Yao, M. Xu, C. Choi, D. J. Crandall, E. M. Atkins, and B. Dariush, "Egocentric vision-based future vehicle localization for intelligent driving assistance systems," in *Proc. Int. Conf. Robot. Automat.*, 2019, pp. 9711–9717, doi: 10.1109/ICRA.2019.8794474.

[29] M. Lüy, E. Cam, F. Ulamis, I. Uzun, and S. Akin, "Initial results of testing a multilayer laser scanner in a collision avoidance system for light rail vehicles," *Appl. Sci.*, vol. 8, no. 4, Mar. 2018, Art. no. 475, doi: 10.3390/app8040475.

[30] F. Fioretti, E. Ruffaldi, and C. A. Avizzano, "A single camera inspection system to detect and localize obstacles on railways based on manifold Kalman filtering," in *Proc. IEEE 23rd Int. Conf. Emerg. Technol. Factory Automat.*, 2018, pp. 768–775, doi: 10.1109/ETFA.2018.8502651.

[31] F. Thullier, A. Beaulieu, J. Maître, S. Gaboury, and K. Bouchard, "A systematic evaluation of the XeThru X4 ultra-wideband radar behavior," *Procedia Comput. Sci.*, vol. 198, pp. 148–155, Jan. 2022, doi: 10.1016/j.procs.2021.12.222.

[32] K. Bouchard, J. Maitre, C. Bertuglia, and S. Gaboury, "Activity recognition in smart homes using UWB radars," *Procedia Comput. Sci.*, vol. 170, pp. 10–17, Jan. 2020, doi: 10.1016/j.procs.2020.03.004.

[33] Q. Deng, J. Le, S. Barbat, R. Tian, and Y. Chen, "Efficient living subject localization and weak vital-sign signal enhancement using impulse radio based UWB radar," in *Proc. IEEE Intell. Veh. Symp. (4th)*, 2019, pp. 777–782, doi: 10.1109/IVS.2019.8814004.

[34] S. Liu, L. Liu, J. Tang, B. Yu, Y. Wang, and W. Shi, "Edge computing for autonomous driving: Opportunities and challenges," *Proc. IEEE*, vol. 107, no. 8, pp. 1697–1716, Aug. 2019, doi: 10.1109/JPROC.2019.2915983.

[35] L. Do, I. Herman, and Z. Hurák, "V2V communication-based rail collision avoidance system for urban light rail vehicles," 2020, *arXiv:200602480.*

[36] Z. Xiao, Y. Hei, Q. Yu, and K. Yi, "A survey on impulse-radio UWB localization," *Sci. China Inf. Sci.*, vol. 53, no. 7, pp. 1322–1335, Jul. 2010, doi: 10.1007/s11432-010-3102-1.

[37] N. Patwari, J. N. Ash, S. Kyperountas, A. O. Hero, R. L. Moses, and N. S. Correal, "Locating the nodes: Cooperative localization in wireless sensor networks," *IEEE Signal Process. Mag.*, vol. 22, no. 4, pp. 54–69, Jul. 2005, doi: 10.1109/MSP.2005.1458287.

[38] I. Domuta and T. P. Palade, "Two-way ranging algorithms for clock error compensation," *IEEE Trans. Veh. Technol.*, vol. 70, no. 8, pp. 8237–8250, Aug. 2021, doi: 10.1109/TVT.2021.3096667.

[39] M. Malajner, P. Planinšič, and D. Gleich, "UWB ranging accuracy," in *Proc. Int. Conf. Syst., Signals Image Process.*, 2015, pp. 61–64, doi: 10.1109/IWSSIP.2015.7314177.

[40] Z. Wang, Y. Khatavkar, R. James, X. Liu, and P. Spasojevic, "Applications of ultra-wideband in future guideway transportation industry: Position paper for north America rail context," in *Proc. 17th Int. Conf. Automated People Movers Automated Transit Syst.*, 2020, pp. 73–84, doi: 10.1061/9780784483077.008.

[41] ETSI, "Intelligent transport systems (ITS)—Vehicular communications—Basic set of applications—Part 2: Specification of cooperative awareness basic service," 2014. [Online]. Available: https://www.etsi.org/deliver/etsi_en/302600_302699/30263702/01.03.02_60/en_30263702v010302p.pdf

[42] Metrom Rail, "FTA Tracs Presentation: AURA Train Control System & Integrated Worker Protection Function," presented at the transit advisory committee for safety (TRACS) technology presentations, Feb. 2020. Accessed: Feb. 08, 2022. [Online]. Available: https://www.transit.dot.gov/sites/fta.dot.gov/files/docs/regulations-and-programs/safety/147776/tracs-technology-presentation-february-2020.pdf

[43] J. Mao et al., "A hybrid reader transceiver design for industrial internet of things," *J. Ind. Inf. Integration*, vol. 2, pp. 19–29, Jun. 2016, doi: 10.1016/j.jii.2016.05.001.

[44] B. Zhen, H.-B. Li, and R. Kohno, "Clock management in ultra-wideband ranging," in *Proc. 16th IST Mobile Wireless Commun. Summit*, 2007, pp. 1–5, doi: 10.1109/ISTMWC.2007.4299163.

[45] Decawave, "DWM1001 system overview and performance version 2.0," 2021. Accessed: Nov. 7, 2023. [Online]. Available: https://www.qorvo.com/products/d/da007974

[46] FCC, "Revision of part 15 of the commission's rules regarding ultra WideBand transmission systems," 2002. [Online]. Available: https://www.fcc.gov/document/revisionpart-15-commissions-rules-regarding-ultra-wideband-7

[47] Decawave, "DW1000 product brief," 2013. Accessed: Feb. 26, 2022. [Online]. Available: https://decaforum.decawave.com/uploads/short-url/93FWaTMGCw3DSbyPD1qixmOj4jB.pdf

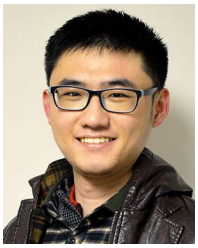

Zezhou Wang (Student Member, IEEE) received the M.S. degree in civil engineering from the University of Illinois at Urbana Champaign, Champaign, IL, USA, in 2018. He is currently working toward the Ph.D. degree in civil engineering with Rutgers University, New Brunswick, NJ, USA, and also working toward the dual-master's degree majored in electrical and computer engineering. His research interests include railway cyber security, signaling and communications, railway ITS, and train control.

Predrag Spasojevic (Member, IEEE) received the Diploma of Engineering from the School of Electrical Engineering, University of Sarajevo, Sarajevo, Bosnia and Herzegovina, in 1990, and the M.S. and Ph.D. degrees from Electrical Engineering, Texas AM University, College Station, TX, USA, in 1992 and 1999, respectively. Since 2001, he has been a Member of the WINLAB and ECE faculty. From 2017 to 2018, he was a Senior Research Fellow with Oak Ridge Associated Universities working with the Army Research Lab, Adelphi, MD, USA. His research interests include the general areas of communication and information theory, and signal processing. Dr. Spasojevic was an Associate Editor for the IEEE COMMUNICATIONS LETTERS from 2002 to 2004 and was the Co-Chair of the DIMACS Princeton-Rutgers Seminar Series in Information Sciences and Systems during 2003–2004. He was a Technical Program Co-Chair of IEEE Radio and Wireless Symposium in 2010. From 2008 to 2011, he was the Publications Editor of the IEEE TRANSACTIONS OF INFORMATION THEORY. He is a Technical Program Track Co-Chair of IEEE Vehicular Technology Conference 2020-Spring and as a Workshop Co-Chair of Game-Theoretic and Behavioral Analysis for Security 2020-Spring.

Bryan W. Schlake received the B.S. degree in mechanical engineering and the M.S. degree in civil and environmental engineering from the University of Illinois at Urbana-Champaign, Champaign, IL, USA, and the Post-graduation degrees in both management and engineering roles from Norfolk Southern Railway, Atlanta, GA, USA. He is currently an Assistant Teaching Professor of rail transportation engineering with Penn State Altoona. His graduate research with the University of Illinois Rail Transportation and Engineering Center (RailTEC) involved analysis of freight car condition monitoring technologies. In addition to investing in the next generation of railroad engineers, Bryan is involved with research related to rolling stock safety, training within industry, and application of lean production principles to railroad mechanical operations.

Ninad Mulay received the B.Tech. degree from the K.J. Somaiya College of Engineering, Mumbai, India. He is currently working toward the graduation degree from the Electrical and Computer Engineering Department, Rutgers University, New Brunswick, NJ, USA. He was with Intel Corporation as an Intern and is currently with VMware as a Software Engineer. His research interests include wireless communications, and COVID contact tracing.

Asim F. Zaman received the M.S. degree in railroad engineering. He is currently a Project Engineer with the Rutgers Center for Advanced Infrastructure and Transportation. He was with the New Jersey Department of Transportation as a Senior Engineer and has more than eight years of experience in transportation engineering and project management. His research interests development of AI and edge computing algorithms and hardware for railroad applications. He received the Dwight D. Eisenhower Transportation Fellowship in 2020 for his research using Artificial Intelligence to detect trespassing in the railroad industry.

Xiang Liu is currently an Associate Professor with the Department of Civil and Environmental Engineering, Rutgers University, New Brunswick, NJ, USA. He is also the Director of the Rutgers Rail and Transit Program, leading and managing a portfolio of rail-centric research, education, and workforce development initiatives. Dr. Liu has authored or coauthored more than 100 papers in peer-reviewed journals and international conferences. His research focuses on developing and testing advanced technologies for improving rail operational safety and efficiency. Dr. Liu's rail & transit research has been supported by a variety of public and private sectors in the United States. Dr. Liu is an Associate Editor for the *Journal of Rail Transport Planning & Management*, and *Journal of Smart and Resilient Transportation*.